Reversion to virulence following infection with a low pathogenicity, CXCR4-dependent molecular clone of feline immunodeficiency virus.

Running title: Reversion to virulence of an apathogenic FIV isolate

MARGARET J. HOSIE[1*], BRIAN J. WILLETT[1], DIETER KLEIN[2],
THOMAS H. DUNSFORD[1],CELIA CANNON[1],
MASAYUKI SHIMOJIMA[3] & OSWALD JARRETT[1].

[1]*Department of Veterinary Pathology, University of Glasgow, Bearsden Road, Glasgow G61 1QH, UK.*
[2]*Institute of Virology, University of Veterinary Medicine, A-1210 Vienna, Austria.*
[3]*Department of Veterinary Microbiology, Graduate School of Veterinary Medicine, University of Tokyo, Japan.*

* corresponding author
Dr. M.J.Hosie
Retrovirus Research Laboratory
Department of Veterinary Pathology
University of Glasgow
Bearsden Road
Glasgow G61 1QH
United Kingdom

E-mail: m.hosie@vet.gla.ac.uk
Tel: +44 141 330 3274, Fax: +44 141 330 5602

SUMMARY

The development of an effective vaccine against human immunodeficiency virus (HIV) is considered to be the most practicable means of controlling the advancing global AIDS epidemic. Studies in the domestic cat have demonstrated that vaccinal immunity to infection can be induced against feline immunodeficiency virus (FIV), however, protection is largely restricted to laboratory strains of FIV and does not extend to primary strains of the virus. We compared the pathogenicity of two prototypic vaccine challenge strains of FIV derived from molecular clones; the laboratory strain PET_{F14} and the primary strain $GL8_{414}$. PET_{F14} established a low viral load and had no effect on CD4+ or CD8+ lymphocyte subsets. In contrast, $GL8_{414}$ established a high viral load and induced a significant reduction in ratio of CD4+ to CD8+ lymphocytes by 15 weeks post infection, suggesting that PET_{F14} may be a low virulence challenge virus. However, during long-term monitoring of the PET_{F14}-infected cats, we observed the emergence of variant viruses in two of three cats. Concomitant with the appearance of the variant viruses, designated 627_{W135} and $628_{W135,}$ we observed an expansion of CD8+ lymphocyte subpopulations expressing reduced CD8β-chain, a phenotype consistent with activation. The variant viruses both carried mutations that reduced the net charge of the V3 loop (K409Q and K409E), giving rise to a reduced ability of the Env proteins to both induce fusion and to establish productive infection in CXCR4-expressing cells. Further, following subsequent challenge of naïve cats with the mutant viruses, the viruses established higher viral loads and induced more marked alterations in CD8+ lymphocyte subpopulations than the parent F14 strain of virus, suggesting that the E409K mutation in the PET_{F14} strain contributes to the attenuation of the virus.

INTRODUCTION

Infection of the domestic cat with feline immunodeficiency virus (FIV) leads to the development of an immunodeficiency syndrome similar to AIDS in human beings infected with human immunodeficiency virus (HIV). FIV-infected cats are more likely to develop illnesses including gingivitis, stomatitis, lymphoma, neurological disorders and wasting (15;24). Flow cytometric analyses have demonstrated a reduction in the number of circulating CD4+ lymphocytes in FIV-infected cats (1;22) and longitudinal studies have revealed that the degree of immune impairment correlates with the decline in $CD4^+$ lymphocyte numbers (34), suggesting that, as with HIV infection in man, the primary lesion in the FIV infected cat is an impairment of helper T-cell function. During the early, acute phase of infection, the inversion of the CD4:CD8 ratio is compounded by a sharp increase in $CD8^+$ T-lymphocytes expressing low levels of CD8 ($CD8^{low}$) and increased levels of major histocompatibility (MHC) class II antigens (39). This activated T-cell subpopulation persists throughout the course of the infection, suggesting that the early interaction between the virus and the immune system may ultimately determine the outcome of the infection. CD8low cells have since been defined as $CD8\alpha+\beta^{low}$ (28;29); the vpg9 antibody used in previous studies being shown to recognise the $CD8\alpha\beta$ heterodimer. An analogous population has since been described in HIV-infected individuals in whom reduced expression of the $CD8\alpha\beta$ heterodimer correlates with increased expression of molecules associated with lymphocyte activation, adhesion and cytotoxic T cell activity (27).   Further, a significant increase in expression of the $CD8\alpha\beta$ heterodimer followed initiation of highly active antiretroviral therapy (HAART) suggesting that analysis of discrete CD8+ T lymphocyte subsets may be of value in assessing the immune status of individuals infected with HIV-1 (27).

Previously, we demonstrated that vaccination with whole-inactivated virus vaccines or DNA vaccines afforded protection against challenge with the cell culture-adapted PET strain of FIV but not against the primary GL8 strain (10;12;13). The induction of protective immunity against primary strains of FIV such as GL8 has proved difficult; outcomes ranged from a suppression of the PBMC viral load and CD4+ T cell loss with a whole inactivated virus vaccine (12), to enhancement of infection following immunisation with FIV p24-ISCOMS (14). Encouragingly,

protective immunity has been induced following immunisation with a fixed, infected cell vaccine based on the MBM cell line (19) and, in field studies, this vaccine provided immunity to infection following natural exposure to the virus (20).   The success of the fixed cell vaccine may be associated with the observation that the vaccine was based on cells infected with a clade B virus strain (Pisa M2), and the vaccine was tested in a region in which clade B viruses are almost exclusively found (20;25). Previous studies have suggested that clade B viruses such as Pisa M2 may be more ancient and relatively host-adapted while clade A viruses may have entered their host population more recently and thus may be more virulent (2;25). As clade A viruses are widespread in the USA and Northern Europe, it is important to establish the determinants of virulence in these viruses.

Cell culture-adapted strains of FIV such as PET differ from primary strains of FIV in that they have an expanded cell tropism that permits growth in established cell lines such as Crandell feline kidney cells (CrFK) or 3201 cells. The underlying mechanism for the expanded cell tropism involves an increase in charge of the V3 loop of the viral envelope glycoprotein (Env) gp120 (31;36). This increase in charge of the V3 loop facilitates the usage feline CXCR4 as a sole receptor for infection (11;37;41;42), possibly in conjunction with heparan sulphate (5) and analogous to CD4-independent infection with HIV-2 (8). In contrast, while infection with most primary strains of FIV is CXCR4-dependent (7;26), the existence of an, as yet, unidentified high affinity non-CD4 primary receptor has been suggested (5;38).

In this study, we compared the virulence of two prototypic clade A vaccine challenge strains of FIV derived from stable molecular clones, PET_{F14} and $GL8_{414}$. We demonstrate that the $GL8_{414}$ molecular clone has similar virulence characteristics to the biological isolate of the virus from which it was derived, establishing a high viral load and inducing marked alterations in circulating CD4+ and CD8+ lymphocyte sub-populations. In contrast, the PET_{F14} virus established a low viral load and had little effect on the CD4+ and CD8+ lymphocyte sub-populations. Further, we show that the emergence of more virulent strains of PET_{F14} *in vivo* is associated with alterations in the way the virus uses CXCR4 as a receptor for infection.

MATERIALS AND METHODS

Viruses and cell lines. All cell culture media and supplements were obtained from Invitrogen Life Technologies Ltd., Paisley, UK. Adherent cell lines were maintained in Dulbecco's modification of minimum essential medium (DMEM) supplemented with 10% foetal bovine serum (FBS), 2mM glutamine, 0.11mg/ml sodium pyruvate, 100 IU/ml penicillin and 100 μg/ml streptomycin (DMEM). The IL2-dependent feline T cell line Mya-1 (21) and peripheral blood mononuclear cells were maintained in RPMI1640 medium supplemented with 10% FBS, 2mM glutamine, 100 IU/ml penicillin,100 μg/ml streptomycin, 5 x 10^{-5} M 2-mercaptoethanol and 100IU/ml recombinant human interleukin 2 (RPMI).

The challenge viruses were prepared from the GL8$_{414}$ (12) and PET$_{F14}$ (33) molecular clones of FIV. Molecular clones were transfected in the murine fibroblast cell line 3T3 using Superfect transfection reagent (QIAgen, Valencia,CA.). 72 hours post transfection, supernatants were harvested, 0.45μm filtered and used to infect the IL2-dependent feline T cell line Q201 (40). The infected cultures were monitored visually for cytopathicity and for the production of FIV p24 by enzyme-linked immunosorbent assay (ELISA, PetCheck FIV antigen ELISA, IDEXX Corp., Portland, Maine, USA). Supernatants were collected at peak cytopathicity/ p24 production, 0.45μm filtered, dispensed into 1ml aliquots and stored at –70°C.

Quantification of proviral load in peripheral blood mononuclear cells. The FIV proviral load in PBMC was quantified using real-time PCR measuring PCR product accumulation through a dual-labeled fluorogenic TaqMan probe (9). The primers used were FIV0771f (5'-AGA ACC TGG TGA TAT ACC AGA GAC-3') and FIV1081r (5'-TTG GGT CAA GTG CTA CAT ATT G-3'). The probe used in this system was FIV1010p (5'-FAM-TAT GCC TGT GGA GGG CCT TCC T-TAMRA-3'). The oligonucleotides were designed to detect a variety of FIV A-subtype isolates and have been previously shown to detect FIV-PET, FIV-GL8 and FIV-AM6 with only minor differences in the PCR efficiency (17,18). The 25 μl PCR mixtures contained 10 mM Tris (pH 8.3), 50 mM KCl, 3 mM MgCl$_2$, 200 nM dATP, dCTP, dGTP, 400 nM dUTP, 300 nM of each primer, 200 nM of the fluorogenic probe and 2.5 units of *Taq* DNA polymerase. After the initial denaturation (2 min. at 95°C),

amplification was performed with 45 cycles of 15 sec at 95°C and 60 sec at 60°C. The PCR reaction and the on-line measurement of the emitted fluorescence were performed on a Sequence Detector System ABI 7700 (Applied Biosystems, Foster City, California). The copy number per PCR reaction was calculated by the Sequence Detection Software version 1.6.3 (Applied Biosystems, Foster City, California) utilizing a fourfold dilution series of genomic DNA derived from a CrFK cell line infected with FIV Petaluma. The DNA content per PCR reaction was estimated by a second real-time PCR assay targeting the 18 S rDNA genes (16).

Quantification of viral load in plasma. The FIV viral load in plasma was quantified by real-time RT-PCR using the same primers as in the real-time PCR. The 25 µl RT-PCR reaction mixtures contained 12.5 µl 2x Thermoscript Reaction Mix (Platinum Quantitative RT-PCR Kit, Life Technologies, Karlsruhe, Germany), 300nM of each primer, 200 nM of the fluorogenic probe, 0.5 µl of the Thermoscript Plus/Platinum *Taq* Enzyme mix, 20 U of RNaseOUT (Life Technologies, Karlsruhe, Germany) and 5 µl of the sample. After a reverse transcription step of 30 min. at 60°C followed by a denaturation step (5 min. at 95°C), amplification was performed with 45 cycles of 15 sec at 95°C and 60 sec at 60°C.

Virus isolation. Virus isolation from PBMC by bulk cell culture was performed as described previously (12). PBMC were fractionated from 5ml of whole blood by centrifugation over Ficoll Paque density 1.077g/ml. The separated PBMC were co-cultured with Mya-1 cells in the absence of mitogenic stimulation. We have found that this protocol enables the isolation of both primary and cell culture-adapted strains of FIV and does not exert a selective pressure on the virus that is isolated e.g. Mya-1 cells will support the growth of PET_{F14} and $GL8_{414}$ equally and the viruses harvested from the cells retain their specific cell tropisms.

Antibodies and flow cytometry. Antibodies were used either un-conjugated or as phycoerythrin (PE) or fluorescein isothiocyanate (FITC) conjugates. Anti-feline CD4-FITC (vpg34) and CD8αβ-PE (vpg9) were obtained from Serotec Ltd., Oxford, U.K;

anti-feline CD8α (12A3) from Y. Nishimura, University of Tokyo, Tokyo, Japan; anti-feline CD8β-FITC and PE (FT2) from Southern Biotechnology Ltd., U.S.A. FITC-conjugated anti-feline CD8α (12A3) was prepared using FITC-coupling reagent (Pierce Chemical Co., Rockford, IL) according to the manufacturers instructions. Un-conjugated primary antibodies were detected using FITC or PE-coupled F(ab')$_2$ fragment of sheep anti-mouse IgG whole molecule (Sigma). EDTA anti-coagulated blood was processed for flow cytometric analyses by whole blood lysis as described previously (39). Samples were analysed on a Beckman Coulter Epics Elite flow cytometer and 10,000 events were collected for each sample. Data were analysed using Expo32 ADC software (Applied Cytometry Systems, Sheffield, U.K.).

Molecular cloning and nucleic acid sequencing. DNAs were prepared from positive viral isolations by column chromatography (QIAamp DNA maxiprep kit, Qiagen). DNAs were prepared as soon as a positive ELISA test for FIV p24 was recorded, thus viruses had undergone minimal passage *in vitro*. Full length viral envelope glycoprotein (*env*) genes were amplified from the replication competent viruses by using a high fidelity (proof reading) polymerase chain reaction (High Fidelity PCR system, Roche) using primers corresponding to the 5' L-SU cleavage site (TAGACGCGTAAGATTTTTAAGGTATTC) and the *Nde*I site 3' of the RRE (CCCTTTGAGGAAGATGTGTCATATGAATCCATT) incorporating *Mlu*I and *Nde*I restriction sites respectively . Due to the inherent instability of the full-length *env* genes from primary isolates of FIV such as GL8, standard high copy number PCR product cloning vectors could not be used, thus all amplified *env* gene products were digested with *Mlu*I/*Nde*I and cloned directly into pGL8$_{MYA}$, a molecular clone of FIV-GL8 in the low copy number plasmid pBR328 and in which an *Mlu*I site has been introduced at the L-SU junction. The nucleic acid sequence of three independent clones of each *env* gene were detemined using IRD800 labelled oligonucleotides on an automated sequencer (LI-COR Biosciences, Lincoln, Nebraska, USA).

In vitro expression of *env* genes. The biological function of each *env* gene clone was confirmed by the recovery of infectious virus following transfection and by immunofluorescence detection of the Env glycoprotein with an anti-FIV Env monoclonal antibody (vpg71.2). For the recovery of infectious virus, 293T cells were

transfected using Superfect (QIAgen) as per manufacturers instructions. Supernatants were collected 48-72hrs post transfection, filtered at 0.45μm and added to Mya-1 cells. The infected cells were monitored for the production of FIV using the PetCheck FIV antigen ELISA (IDEXX Corp., Portland, Maine, USA).

Immunofluorescence was performed on transfected 293T cells following fixation with ice-cold methanol. Fixed cells were re-hydrated using phosphate buffered saline containing 1.0% bovine serum albumin and 0.1% azide (PBA). The cells were then incubated with either 1μg of vpg71.2 or an isotype-matched control for 30 minutes on ice, washed twice with PBA by centrifugation, and then incubated with FITC-coupled F(ab')$_2$ fragment of sheep anti-mouse IgG whole molecule on ice for a further 30 minutes. Finally, the cells were washed twice with PBA and then analysed on a Leica UV microscope.

To assess the fusogenicity of the FIV Env proteins, the *env* genes were sub-cloned into the mammalian expression vector VR1012 (Vical Incorporated, San Diego, CA.). AH927 cells expressing feline CXCR4 were transfected with the constructs using Superfect (Qiagen) and incubated for 48 hours at 37°C. The cells were then fixed and stained with 1% methylene blue/ 0.2% basic fuchsin in methanol. Syncytia were enumerated by light microscopy using a x12.5 Leitz periplan eyepiece with a 6.5x9 graticule, three separate fields being counted per well, each well in duplicate. Syncytia were scored as cells with five or more nuclei.

The growth of FIV *in vitro* was assessed in AH927 cells expressing feline CXCR4. AH927 cells were transduced with retroviral vectors (pDONAI, Takara Biotech., Japan) expressing feline CXCR4 or CCR5 and selected in G418. Stable transfectants were seeded in 48-well cell culture plates and were then infected with two-fold dilutions of virus grown in IL2-dependent T cells. Supernatants were collected every three days and assayed for the production of reverse transcriptase (RT) using Lenti-RT non-isotopic RT assay kit (Cavidi Tech., Uppsala, Sweden). RT values were then calculated relative to purified HIV-1 RT standard.

RESULTS

Early infection

FIV GL8 rapidly establishes a high viral load. Three groups of three cats were infected with either a matched dose of FIV $GL8_{414}$ or PET_{F14}, or were mock-infected. Samples of peripheral blood were collected at regular intervals after infection and the PBMC proviral DNA burden was quantified by real-time PCR (Fig. 1a). The proviral loads in the $GL8_{414}$-infected cats rose sharply with approximately 1.0% of PBMC being positive for proviral DNA by 6 weeks post infection. This high proviral burden was maintained throughout the acute phase of infection, and during the first 35 weeks of the study period. In contrast, the PET_{F14} inoculum established a significantly lower proviral load, with a load of approximately 0.01% being achieved during the acute phase (Fig 1a). During this period, the effect of viral infection on the CD4:CD8 ratio was monitored by flow cytometry. Coincident with the sharp rise in proviral load in the $GL8_{414}$ infected cats was a marked decline in the CD4:CD8 ratio manifesting by six weeks post infection (Fig1b). In contrast, the CD4:CD8 ratios of the PET_{F14} infected cats did not differ significantly from the controls.

Expansion of CD8α+/β^{low} T lymphocytes in $GL8_{414}$-infected cats. Previously, we demonstrated that the biological isolate of GL8 induced rapid alterations in the CD8+ lymphocyte subset characterised by reduced expression of CD8 (CD8^{low}) (39). Subsequently, the CD8^{low} population was revealed to consist of CD8$\alpha\beta^{low}$ and CD8$\alpha\alpha$' populations (28;29), analogous to the population described in HIV-infected individuals (27). The absolute numbers of CD4+, CD8+ and CD8$\alpha\beta^{low}$ were determined in the three groups of cats (Fig.2). CD4+ lymphocyte numbers dropped sharply in both the $GL8_{414}$ and PET_{F14}–infected cats at 3 weeks post infection. However this proved to be a transient fall as the levels rebounded by 6 weeks post infection. Although the data suggest that there was a downward trend in the CD4+ lymphocyte numbers in both the FIV-infected groups it was not until 67 weeks post infection that the reduction in the CD4+ lymphocyte number in the $GL8_{414}$-infected cats reached statistical significance (P=0.046, t-test). The major contributing factor to the depressed CD4:CD8 ratio in the $GL8_{414}$-infected cats was a transient, sharp increase in the number of CD8+ lymphocytes (Fig. 2b). When the analysis gates for

flow cytometry are focussed on the $CD8\alpha\beta^{low}$ subset (Fig. 2c), it can be seen that this population expands by 9 weeks post infection to a maximum of $1.0x10^9/l$, returning to pre-infection levels ($<0.4x10^9/l$) by 32 weeks post infection. Due to the small numbers of cats in each group the elevated numbers of $CD8\alpha\beta^{low}$ lymphocytes did not reach statistical significance. In contrast to the $GL8_{414}$-infected cats, $CD8\alpha\beta^{low}$ lymphocytes could not be detected at any of the time points during the acute phase of infection in the PET_{F14}-infected cats. The data indicate that the virus derived from the $GL8_{414}$ molecular clone is as pathogenic as the original biological isolate of GL8 and that cats infected with the $GL8_{414}$ or PET_{F14} viruses can be differentiated readily on the basis of viral load. Further, at no point during the early acute phase of infection did we observe the $CD8\alpha\beta^{low}$ subset in PET_{F14}-infected cats, consistent with the this subset being a marker for infection with a more pathogenic strain of FIV, such as $GL8_{414}$.

Long-term infection

Emergence of pathogenic variants of FIV_{F14} during prolonged infection.
Throughout the acute phase of infection, virus could be isolated readily *in vitro* from PBMC cultures from both groups of infected cats (data not shown). By 32 weeks post infection, virus isolation became sporadic from the PET_{F14}-infected cats, consistent with the low viral loads indicated by real-time PCR (Fig. 1). In contrast, virus could be isolated readily from $GL8_{414}$-infected cats at all time points (data not shown). These findings may indicate that the immune response to infection was limiting the replication of PET_{F14}, but not of $GL8_{414}$ and are consistent with the contention that the PET_{F14} virus is less virulent than $GL8_{414}$. Following the early peak in viral load during the acute phase of infection, the proviral burden in the PBMC of the PET_{F14}-infected cats fell below the level of assay sensitivity. In contrast, a high proviral burden was maintained in the $GL8_{414}$-infected cats throughout the study period (Figure 3).

By 144 weeks post infection bulk virus isolations from PBMCs from cats 627 and 628 tested positive, despite the PBMC proviral load remaining below assay sensitivity ($<1x10^{-5}$ % infected PBMC). Coincident with the positive virus isolations, we observed the expansion of the $CD8\alpha\beta^{low}$ subset in the same cats (Figure 4). As we had not observed an expansion of $CD8\alpha\beta^{low}$ subset in the PET_{F14}-infected cats at any

time point during the acute phase of infection, we postulated that virulent escape mutants may have evolved with time post infection.

Characterisation of the emergent virus strains from PET$_{F14}$-infected cats. Virus was isolated from peripheral blood mononuclear cells from cats A627 and A628 and the *env* genes amplified by high-fidelity PCR and cloned. The nucleic acid sequence of the *env* clones was then determined and the predicted amino acid sequence translation established. Fig.5 illustrates the predicted amino acid sequence of the Env region from V3 through to V6, a region that has been shown previously to contain determinants of cell tropism (31;36) and CXCR4 usage (5;42). The mutation of either of two glutamate residues in V3 (residues 407 and 409 in GL8$_{414}$ in Fig. 5) to lysine residues is thought to determine the usage of CXCR4 as a sole receptor (analogous to CD4-independent infection with HIV). The PET$_{F14}$ virus contains a lysine residue at position 409. In the virus re-isolated from cats 628 at 135 weeks post infection (628$_{W135}$), lysine 409 had been replaced with a glutamate residue (K409E), analogous to GL8$_{414}$ which reduces the net charge of the V3 loop by replacing a positively charged residue with a negatively charged residue. A second coding mutation (S557N) observed in the re-isolate from cat 628 introduced a predicted N-linked glycosylation site in the V5 region. Intriguingly, the week 135 re-isolate from cat 627 (627$_{W135}$) also showed a mutation at position 409 in the V3 loop (K409Q), replacing a positively charged residue with a neutral residue, again reducing the net charge of the V3 loop. A second mutation (N422T) removed a predicted site for N-linked glycosylation from the region at the base of the V3 loop. Given that the glutamate residues 407 and 409 are known to be critical determinants of the interaction between FIV and CXCR4, the data suggest that there may be a direct link between CXCR4-usage and virulence.

Given that changes in the TM protein of FIV affect cell tropism (35), we compared the sequences of the TM protein of the 627$_{W135}$ and 628$_{W135}$ clones with the parent PET$_{F14}$. The TM sequence of 628$_{W135}$ Env showed no changes from the parental virus while the TM sequence of 627$_{W135}$ showed two coding mutations distinct from those described previously to affect cell tropism. As these changes were not common to the 627$_{W135}$ and 628$_{W135}$ viruses they are unlikely to be responsible for the reversion to a virulent phenotype. Similarly, of the changes observed in the region of SU between the L-SU cleavage site and V3, only a conservative change F208L,

was observed in both 627_{W135} and 628_{W135}. 628_{W135} displayed additional $T_{154}K$ (neutral hydrophilic to basic) and R252G (basic to amphiphilic) changes, while an additional F388L (conservative) substitution was detected in 627_{W135}.

In vitro properties of the reverted viruses. E407K and E409K substitutions in the V3 loop of FIV SU alone are sufficient to permit infection of CrFK cells with FIV and CrFK-tropic viruses bind CXCR4 with a high affinity (31). Data presented to date suggest that infection of adherent cell lines such as CrFK cells requires an interaction between the viral envelope glycoprotein and CXCR4 (5;11;42) and heparan sulphate (5), indeed ectopic expression of CXCR4 is sufficient to render cells permissive for syncytia formation and cell-free virus infection with CrFK-adapted strains of FIV (viruses carrying E to K mutations in the V3 loop) (36;37;42). In contrast, ectopic expression of feline CXCR4 or CCR5 does not render cells permissive to infection with primary strains of FIV such as GL8, leading to the proposal the primary strains utilise an as yet unidentified high affinity binding receptor for infection of primary IL2-dependent T cells (37). Recent compelling evidence revealed that recombinant FIV envelope glycoproteins bind distinct cell surface molecules on lymphoid cell lines compared with adherent cell lines, further implicating a high affinity primary binding receptor for attachment to these cell lines (5). The PET_{F14} virus represents a CrFK-adapted strain of FIV, the viral envelope glycoprotein binds to CXCR4 with a high affinity and expression of the envelope glycoprotein alone in CXCR4-expressing cells promotes syncytium-formation (11;37). We therefore assessed the *in vitro* properties of the PET_{F14} revertant viruses 627_{W135} and 628_{W135} in comparison with the parental PET_{F14} virus, the $GL8_{414}$ virus, and a mutant GL8 envelope glycoprotein bearing an E407K mutation ($GL8_{E407K}$). DNAs encoding the envelope glycoproteins were sub-cloned into a mammalian expression vector (VR1012) and transfected directly into the feline cell line AH927 stably expressing feline CXCR4 (Fig.6) or CCR5 (not shown). Marked syncytium formation was observed in the cultures transfected with the PET_{F14} *env* construct (Fig. 6a.), the syncytia often being large (>20 nuclei per syncytium, 30+/-2 per field). In contrast, the number of syncytia in the $GL8_{414}$-transfected cultures (0.2+/-0.2 per field) did not differ from the cultures transfected with the vector alone (0.2 +/- 0.2 per field). The 627_{W135} and 628_{W135} *env* genes gave an intermediate phenotype, with fewer, smaller syncytia (5-10 nuclei per syncytium, 2.4+/-1.5 per field and 4.4+/-2.3 per field respectively). The $GL8_{E407K}$

mutant gave a similar size and number of syncytia to the 627_{W135} and 628_{W135}. No syncytia were observed in AH927 cells stably expressing feline CCR5 following transfection with the envelope constructs (not shown). The data suggest that the observed reduction in net charge of the V3 loop of 627_{W135} and 628_{W135} resulted in an impaired ability to induce syncytia in CXCR4-expressing feline cells compared with the parental PET_{F14} strain. Further, despite having a significantly reduced ability to induce syncytia formation in CXCR4-expressing cells, the retention of a degree of syncytium-forming capacity by the 627_{W135} and 628_{W135} envelope glycoproteins suggest that other regions in the parental PET_{F14} envelope glycoprotein contribute to its highly fusogenic phenotype. Accordingly, while the E407K mutation rendered the GL8 envelope glycoprotein fusogenic, the extent of syncytium formation was markedly lower than that of the PET_{F14} envelope glycoprotein.

The ability to form syncytia in adherent cell lines appears to be dependent on the expression of CXCR4 (41;42) and the binding of recombinant envelope glycoprotein involves an interaction with both CXCR4 and heparan sulphate (5). Therefore we asked whether the reduction in the net charge of the V3 loop of the 627_{W135} and 628_{W135} viruses affected the growth of the viruses in vitro in established cell lines. The PET_{F14}, $GL8_{414}$, 627_{W135} and 628_{W135} viruses were used to infect AH927 cells stably expressing feline CXCR4, since these cells are known to support the growth of viruses carrying an Env protein adapted for growth in cell culture (the use of CXCR4 as a sole receptor), while restricting the growth of viruses carrying primary Env proteins (our unpublished observations). In agreement with the studies on the fusogenicity of the viral Env proteins, AH927-FX4 cells supported the growth of PET_{F14} but not $GL8_{414}$. Growth of the 627_{W135} and 628_{W135} viruses was severely impaired but was detectable (Fig. 7). Furthermore, the CXCR4 antagonist AMD3100 inhibited the growth of the PET_{F14}, 627_{W135} and 628_{W135} viruses (Fig. 7), thus confirming that while infection was less efficient, it was CXCR4-dependent. Infection of AH927-FX4E with the PET_{F14}, 627_{W135} and 628_{W135} viruses was sensitive to pre-treatment of the cells with heparinase (data not shown), suggesting that heparan sulphate may play a role in infection of this cell line with these viruses. These findings are in accord with previous findings in which heparan sulphate was found to be required for binding of recombinant 34TF10 FIV SU to adherent cell lines. As all four viruses grew readily in IL2-dependent T cells (data not shown), the data confirm that the mutations detected in the V3 loop of the 627_{W135} and 628_{W135} viruses lead to a

partial restoration of the characteristics of a primary isolate (loss of the ability to replicate in CXCR4-expressing adherent cell lines). However, the reduced fusogenicity (Fig. 6) and growth (Fig. 7) of the 627_{W135} and 628_{W135} viruses suggests that the viruses harbour determinants outwith the V3-V6 region of Env that are required for efficient replication in these cells.

Virulence of the 627_{W135} and 628_{W135} viruses *in vivo*

The data presented above suggest that the 627_{W135} and the 628_{W135} viruses have reverted to a more pathogenic phenotype than the parental PET$_{F14}$ molecular clone. In order to test this hypothesis, we infected three groups of cats with matched doses of either the PET$_{F14}$, 627_{W135} or 628_{W135} viruses. Our previous data had indicated that the major differences between the GL8$_{414}$ and PET$_{F14}$ viruses were 1) viral load and 2) expansion of CD8+ lymphocyte subpopulations. GL8$_{414}$ achieved a high viral load and triggered an expansion of CD8+ lymphocytes expressing reduced CD8β (CD8βlow) while PET$_{F14}$ achieved a lower viral load and did not affect CD8+ lymphocyte subpopulations. Following infection with the 628_{W135} virus, marked increases in both proviral load (Fig. 8a) and plasma viral load (Fig. 8b) were detected as early as 3 weeks post-infection. These increased proviral and viral loads were mirrored by an expansion of lymphocytes expressing CD8βlow (Fig. 8c). In contrast, while infection with the 627_{W135} virus achieved a similar initial plasma viraemia at 3 weeks post infection, by week 6 the levels of virus in plasma had dropped markedly. Flow cytometric analysis of peripheral blood lymphocytes from these cats revealed a transient increase in lymphocytes expressing CD8βlow at 7 weeks post-infection returning to control levels by 12 weeks post-infection. Infection with PET$_{F14}$ resulted in a transient plasma viraemia at 3 weeks post-infection, returning to baseline levels by 7 weeks post-infection. While a small increase in lymphocytes expressing CD8βlow was observed in the PET$_{F14}$ infected cats at 7 weeks post-infection, the increase was markedly reduced compared to the cats infected with 627_{W135}, and in particular 628_{W135}. Thus infection of naïve cats with the 627_{W135} and 628_{W135} viruses reproduced the alterations observed in the immune systems of cats A627 and A628 with the emergence of the mutant viruses. Further, the infection experiments suggest a correlation between viral load and the expansion of lymphocytes expressing

CD8βlow. The data confirm that the 627_{W135} and 628_{W135} viruses are more pathogenic than the parental PET_{F14} virus.

DISCUSSION

In this study we compared the pathogenicity of two strains of FIV used routinely as challenge strains for vaccine studies. As the viruses were derived from molecular clones, they represent a reproducible source of virus for inter-study comparison. While it is possible to induce protective immunity to infection with the PET isolate (10;43), the $GL8_{414}$ strain represents a more stringent challenge. To date, protective immunity has not been observed against the GL8 isolate of FIV, although a reduction in viral load has been observed following immunisation with a whole inactivated virus vaccine (12). The data presented here suggest that the GL8 strain of FIV is intrinsically more pathogenic than the PET strain of FIV, a strain of virus that has been suggested to be of low pathogenicity (6;12). Using minimally-passaged virus derived from the $GL8_{414}$ molecular clone of FIV, we have established that GL8 achieves a significantly greater viral load in infected cats than PET (approximately 100-fold higher). Further, the $GL8_{414}$-derived virus reproduces the sharp drop in the CD4:CD8 ratio described previously for the biological isolate of GL8 (39) and representative of pathogenic strains of FIV(1;22;44). Having established that the PET_{F14}-derived virus was less virulent than the $GL8_{414}$-derived virus, we followed the two groups of infected cats and noted the emergence of pathogenic variants of PET_{F14} in two of the infected cats 135 weeks after infection (627_{W135} and 628_{W135}). The Env sequences of these viruses displayed characteristic changes in the V3 loop residues that are known to govern the ability of FIV to infect CXCR4-expressing adherent cell lines. Subsequently, we showed that the mutant viruses had a greatly reduced ability to trigger syncytium formation, were less able to establish a productive infection in adherent cells expressing CXCR4 and were more pathogenic than the parental PET_{F14} virus when inoculated *in vivo*.

The reversion from an avirulent (PET_{F14}) to a virulent phenotype (627_{W135} and 628_{W135}) at approximately two years post infection is of particular significance given that "attenuated" laboratory strains of FIV have been suggested as potential vaccines for protection against virulent strains of the virus. Many laboratory strains of FIV display an increase in the net charge of the V3 loop (e.g. PET_{F14}(23), PET_{34TF10} (33), UT113 (36), AM6 (31) and $GL8_{CrFK}$ (37)) analogous to CD4-independent strains of HIV. The increase in charge of the V3 loop correlates with enhanced replication in CXCR4-expressing feline cell lines such as CrFK (31;36). It is thought that such

mutations enable the virus to infect cells in the absence of an as yet unidentified primary receptor (37;38), perhaps by facilitating a direct interaction with CXCR4. Alternatively, it is possible that the decreased net charge of the V3 loop in $A627_{W135}$ and $A628_{W135}$ might result in either a decreased ability of these viruses to adsorb efficiently to the cell surface via heparan sulphate (5). Indeed, it is conceivable that the limited replication of PET_{F14} *in vivo* may result from the virus being trapped on endothelial cells and other tissues expressing large amounts of heparan sulphate on their surface.

Using the PET_{F14} as a typical CXCR4-tropic strain of FIV, we show here that while this phenotype is positively selected *in vitro*, it is not stable *in vivo*. Further, given that PET_{F14} neither established a high viral load nor induced the expansion of activated CD8+ T lymphocyte sub-populations, and the emergence of the variants 627_{W135} and 628_{W135} coincided with the expansion of CD8+ lymphocyte populations and an increased frequency of successful virus isolations, the data suggest that the V3 loop mutation associated with high affinity CXCR4 usage *in vitro* leads to attenuation *in vivo*.

The sequence changes that were detected in the V3 loop of the envelope glycoprotein may have arisen as a result of selection from virus neutralizing antibodies, since this region represents a major neutralizing determinant for FIV. It is possible that the PET_{F14} is more readily neutralizable than the 627_{W135} and 628_{W135} variants, thus accounting for the lower viral load in PET_{F14} infected cats. In previous studies, escape from neutralizing antibodies was correlated with mutations in the V4 or V5 regions of the virus, the emergence of neutralization resistant strains having been examined both *in vitro* and *in vivo* (3;4;30;32). By comparison, however, we did not observe consistent changes in this region of the 627_{W135} and 628_{W135} variants. Neither re-isolate contained mutations in the V4 region and while 628_{W135} had acquired a mutation that would give rise to a predicted N-linked glycosylation site (S557N), this was not present in the 627_{W135} re-isolate. While the additional glycosylation site in V5 of 628_{W135} may confer a replicative advantage to the virus by conferring resistance to neutralising antibodies, this alone was clearly not the main determinant of virulence. In contrast, the K409Q and K409E mutations in the 627_{W135} and 628_{W135} variants are consistent with previous *in vivo* selected variants based on the PET_{34TF10} clone of FIV (3;4). The PET_{34TF10} clone of FIV has lysine residues at

positions 407 and 409 in the V3 loop. However following passage *in vivo*, the re-isolated virus showed K407E and K409G mutations (4).

The emergence of the 627_{W135} and 628_{W135} variants in the PET_{F14}–infected cats correlated well with the appearance of activated CD8+ lymphocyte subpopulations, characterised by reduced expression of CD8β. One of the first indications that more virulent viruses had evolved in cats 627 and 628 was an increased frequency with which virus could be isolated from bulk PBMC cultures. As real-time PCR for proviral DNA load in PBMC during this period remained consistently negative, the data suggest that although the viral load had increased in the cats, the levels of virus were still very low, below the assay sensitivity of $1 \times 10^{-5}\%$ infected PBMC. In contrast, the proviral loads in the $GL8_{414}$-infected cats remained high throughout the study. If the variant viruses in cats 627 and 628 were more virulent than the parental PET_{F14} virus, we would have expected an increased proviral load following the emergence of the variant viruses. The finding that the proviral load remained below the sensitivity of the real-time PCR assay may indicate suppression of viral replication by the host immune response. We addressed this possibility by challenging three groups of naïve cats with either the variants 627_{W135} and 628_{W135}, or the parental virus PET_{F14}. Following challenge, the variant viruses achieved higher viral loads than the parental strain, indicating that in the absence of a pre-existing immune response the viruses were more virulent than the parental strain. Further, infection with the 627_{W135} and 628_{W135} viruses induced a concomitant expansion of CD8βlow lymphocytes.

Further issues to address in the FIV system are the relationship between determinants of virulence *in vitro* and pathogenesis *in vivo*. This study focussed on a comparison of two isolates of FIV that have been used extensively as challenge viruses in vaccine studies. It is not known whether viruses isolated from cats infected in the field are predominantly virulent and pathogenic, similar to $GL8_{414}$, or whether a spectrum of isolates with varying degrees of virulence and pathogenicity exist. It is possible that the virulence characteristics of field isolates depend on the stage of infection. Proviral loads measured in field cats by real-time PCR were comparable to those of cats infected with the $GL8_{414}$ isolate (D.Klein, unpublished data) rather than the low loads detected in cats infected with the PET_{F14} isolate. In future studies, it will be important to examine the virulence characteristics and pathogenicity of field isolates to establish whether particular virulence determinants exist that characterise

the behaviour of FIV isolates *in vivo*. This will enable the selection of vaccine challenge strains that are most representative of field isolates and thus will impact upon future lentiviral vaccine strategies.

ACKNOWLEDGMENTS

REFERENCES

1. **Ackley, C.D., J.K. Yamamoto, N. Levy, N.C. Pedersen, and M.D. Cooper**. 1990. Immunologic abnormalities in pathogen-free cats experimentally infected with feline immunodeficiency virus. J.Virol. **64**:5652-5655.

2. **Bachmann, M.H., C. Mathiason-Dubard, G.H. Learn, A.G. Rodrigo, D.L. Sodora, P. Mazzetti, E.A. Hoover, and J.I. Mullins**. 1997. Genetic diversity of feline immunodeficiency virus: dual infection, recombination, and distinct evolutionary rates among envelope sequence clades. J.Virol. **71**:4241-4253.

3. **Bendinelli, M., M. Pistello, D. Del Mauro, G. Cammarota, F. Maggi, A. Leonildi, S. Giannecchini, C. Bergamini, and D. Matteucci**. 2001. During readaptation in vivo, a tissue culture-adapted strain of feline immunodeficiency virus reverts to broad neutralization resistance at different times in individual hosts but through changes at the same position of the surface glycoprotein. J.Virol. **75**:4584-4593.

4. **Cammarota, G., D. Matteucci, M. Pistello, E. Nicoletti, S. Giannecchini, and M. Bendinelli**. 1996. Reduced sensitivity to strain-specific neutralization of laboratory-adapted feline immunodeficiency virus after one passage in vivo: association with amino acid substitutions in the V4 region of the surface glycoprotein. Aids Res.Hum.Retroviruses **12**:173-175.

5. **de Parseval, A. and J.H. Elder**. 2001. Binding of recombinant feline immunodeficiency virus surface glycoprotein to feline cells: role of CXCR4, cell-surface heparans, and an unidentified non-CXCR4 receptor. J.Virol. **75**:4528-4539.

6. **Dean, G.A., S. Himathongkham, and E.E. Sparger**. 1999. Differential cell tropism of feline immunodeficiency virus molecular clones in vivo. J.Virol. **73**:2596-2603.

7. **Egberink, H.F., E. De Clerq, A.L. Van Vliet, J. Balzarini, G.J. Bridger, G. Henson, M.C. Horzinek, and D. Schols**. 1999. Bicyclams, Selective Antagonists of

the Human Chemokine Receptor CXCR4, Potently Inhibit Feline Immunodeficiency Virus Replication. J.Virol. **73**:6346-6352.

8. **Endres, M.J., P.R. Clapham, M. Marsh, M. Ahuja, J.D. Turner, A. McKnight, J.F. Thomas, B. Stoebenau-Haggarty, S. Choe, P.J. Vance, T.N.C. Wells, C.A. Power, S.S. Sutterwala, R.W. Doms, N.R. Landau, and J.A. Hoxie**. 1996. CD4-independent infection by HIV-2 is mediated by fusin. Cell **87**:745-756.

9. **Heid, C.A., J. Stevens, K.J. Livak, and P.M. Williams**. 1996. Real time quantitative PCR. Genome Res. **6**:986-994.

10. **Hosie, M., R. Osborne, J.K. Yamamoto, J.C. Neil, and O. Jarrett**. 1995. Protection against homologous but not heterologous challenge induced by inactivated feline immunodeficiency virus vaccines. J.Virol. **69**:1253-1255.

11. **Hosie, M.J., N. Broere, J. Hesselgesser, J.D. Turner, J.A. Hoxie, J.C. Neil, and B.J. Willett**. 1998. Modulation of feline immunodeficiency virus infection by stromal cell-derived factor (SDF-1). J.Virol. **72**:2097-2104.

12. **Hosie, M.J., T. Dunsford, D. Klein, B.J. Willett, C. Cannon, R. Osborne, J. Macdonald, N. Spibey, N. Mackay, O. Jarrett, and J.C. Neil**. 2000. Vaccination with inactivated virus but not viral DNA reduces virus load following challenge with a heterologous and virulent isolate of feline immunodeficiency virus. J.Virol. **74**:9403-9411.

13. **Hosie, M.J., J.N. Flynn, M.A. Rigby, C. Cannon, T.H. Dunsford, N.A. Mackay, D. Argyle, B.J. Willett, T. Miyazawa, D.E. Onions, O. Jarrett, and J.C. Neil**. 1998. DNA vaccination affords significant protection against feline immunodeficiency virus infection without inducing detectable antiviral antibodies. J.Virol. **72**:7310-7319.

14.   **Hosie, M.J., R. Osborne, G. Reid, J.C. Neil, and O. Jarrett**. 1992. Enhancement after feline immunodeficiency virus vaccination. Vet.Immunol.Immunopathol. **35**:191-198.

15.   **Hosie, M.J., C. Robertson, and O. Jarrett**. 1989. Prevalence of feline leukaemia virus and antibodies to feline immunodeficiency virus in cats in the United Kingdom. Vet.Rec. **128**:293-297.

16.   **Klein, D., B. Bugl, W.H. Gunzburg, and B. Salmons**. 2000. Accurate estimation of transduction efficiency necessitates a multiplex real-time PCR. Gene Ther. **7**:458-463.

17.   **Klein, D., P. Janda, R. Steinborn, M. Muller, B. Salmons, and W.H. Gunzburg**. 1999. Proviral load determination of different feline immunodeficiency virus isolates using real-time polymerase chain reaction: influence of mismatches on quantification. Electrophoresis **20**:291-299.

18.   **Klein, D., C.M. Leutenegger, C. Bahula, P. Gold, R. Hofmann-Lehmann, B. Salmons, H. Lutz, and W.H. Guenzburg.** 2001. Influence of preassay and sequence variations on viral load determination by a multiplex real-time reverse transcriptase-polymerase chain reaction for feline immunodeficiency virus. J.AIDS **26**:8-20.

19.   **Matteucci, D., M. Pistello, P. Mazzetti, S. Giannecchini, D. Del Mauro, L. Zaccaro, P. Bandecchi, F. Tozzini, and M. Bendinelli**. 1996. Vaccination protects against in vivo-grown feline immunodeficiency virus even in the absence of detectable neutralising antibodies. J.Virol. **70**:617-622.

20.   **Matteucci, D., A. Poli, P. Mazzetti, S. Sozzi, F. Bonci, P. Isola, L. Zaccaro, S. Giannecchini, M. Calandrella, M. Pistello, S. Specter, and M. Bendinelli**. 2000. Immunogenicity of an anti-clade B feline immunodeficiency fixed-cell virus vaccine in field cats. J.Virol. **74**:10911-10919.

21.   **Miyazawa, T.M., T. Furuya, S. Itagaki, Y. Tohya, E. Takahashi, and T. Mikami**. 1989. Establishment of a feline T-lymphoblastoid cell line highly sensitive for replication of feline immunodeficiency virus. Arch.Virol. **108**:131-135.

22.   **Novotney, C., R.V. English, J. Housman, M.G. Davidson, M.P. Nasisse, C.R. Jeng, W.C. Davis, and M.B. Tompkins**. 1990. Lymphocyte population changes in cats naturally infected with feline immunodeficiency virus. AIDS **4**:1213-1218.

23.   **Olmsted, R.A., A.K. Barnes, J.K. Yamamoto, V.M. Hirsch, R.H. Purcell, and P.R. Johnson**. 1989. Molecular cloning of feline immunodeficiency virus. Proc.Natl.Acad.Sci.USA **86**:2448-2452.

24.   **Pedersen, N.C., E.W. Ho, M.L. Brown, and J.K. Yamamoto**. 1987. Isolation of a T-lymphotropic virus from domestic cats with an immunodeficiency syndrome. Science **235**:790-793.

25.   **Pistello, M., G. Cammarota, E. Nicoletti, D. Matteucci, M. Curcio, D. Del Mauro, and M. Bendinelli**. 1997. Analysis of the genetic diversity and phylogenetic relationship of Italian isolates of feline immunodeficiency virus indicates a high prevalence and heterogeneity of subtype B. J.Gen.Virol. **78**:2247-2257.

26.   **Richardson, J., G. Pancino, T. Leste-Lasserre, J. Schneider-Mergener, M. Alizon, P. Sonigo, and N. Heveker**. 1999. Shared usage of the chemokine receptor CXCR4 by primary and laboratory adapted strains of feline immunodeficiency virus. J.Virol. **73**:3661-3671.

27.   **Schmitz, J.E., M.A. Forman, M.A. Lifton, O. Concepcion, K.A.J. Reimann, C.S. Crumpacker, J.F. Daley, R.S. Gelman, and N.L. Letvin**. 1998. Expression of the CD8alpha beta-heterodimer on CD8(+) T lymphocytes in peripheral blood lymphocytes of human immunodeficiency virus- and human immunodeficiency virus+ individuals. Blood **92**:198-206.

28.   **Shimojima, M., T. Miyazawa, M. Kohmoto, Y. Ikeda, Y. Nishimura, K. Maeda, Y. Tohya, and T. Mikami**. 1998. Expansion of CD8alpha+beta- cells in cats infected with feline immunodeficiency virus. J.Gen.Virol. **79**:91-94.

29.   **Shimojima, M., M.R. Pecoraro, K. Maeda, Y. Tohya, T. Miyazawa, and T. Mikami**. 1998. Characterization of anti-feline CD8 monoclonal antibodies. Vet.Immunol.Immunopathol. **61**:17-23.

30.   **Siebelink, K.H.J., W. Huisman, J.A. Karlas, G.F. Rimmelzwaan, M.L. Bosch, and A.D.M.E. Osterhaus**. 1996. Neutralization of feline immunodeficiency virus by polyclonal feline antibody: simultaneous involvement of hypervariable regions 4 and 5 of the surface glycoprotein. J.Virol. **69**:5124-5127.

31.   **Siebelink, K.H.J., J.A. Karlas, G.F. Rimmelzwaan, A.D.M.E. Osterhaus, and M.L. Bosch**. 1995. A determinant of feline immunodeficiency virus involved in CrFK tropism. Vet.Immunol.Immunopathol. **46**:61-69.

32.   **Siebelink, K.H.J., G.F. Rimmelzwaan, M.L. Bosch, R.H. Meloen, and A.D.M.E. Osterhaus**. 1993. A single amino acid substitution in hypervariable region 5 of the envelope protein of feline immunodeficiency virus allows escape from virus neutralisation. J.Virol. **67**:2202-2208.

33.   **Talbott, R.L., E.E. Sparger, K.M. Lovelace, W.M. Fitch, N.C. Pedersen, P.A. Luciw, and J.H. Elder**. 1989. Nucleotide-sequence and genomic organization of feline immunodeficiency virus. Proceedings Of The National Academy Of Sciences Of The United States Of America **86**:5743-5747.

34.   **Torten, M., M. Franchini, J.E. Barlough, J.W. George, E. Mozes, H. Lutz, and N.C. Pedersen**. 1991. Progressive immune dysfunction in cats experimentally infected with feline immunodeficiency virus. J.Virol. **65**:2225-2230.

35.   **Vahlenkamp, T.W., E.J. Verschoor, N.N.M.P. Schuurman, A.L.W. van Vliet, M.C. Horzinek, H.F. Egberink, and A. de Ronde**. 1997. A single amino acid

substitution in the transmembrane envelope glycoprotein of feline immunodeficiency virus alters cellular tropism. J.Virol. **71**:7132-7135.

36.   **Verschoor, E.J., L.A. Boven, H. Blaak, A.R.W. van Vliet, M.C. Horzinek, and A. de Ronde**. 1995. A single mutation within the V3 envelope neutralization domain of feline immunodeficiency virus determines its tropism for CRFK cells. J.Virol. **69**:4752-4757.

37.   **Willett, B.J., K. Adema, N. Heveker, A. Brelot, L. Picard, M. Alizon, J.D. Turner, J.A. Hoxie, S. Peiper, J.C. Neil, and M.J. Hosie**. 1998. The second extracellular loop of CXCR4 determines its function as a receptor for feline immunodeficiency virus. J.Virol. **72**:6475-6481.

38.   **Willett, B.J. and M.J. Hosie**. 1999. The role of the chemokine receptor CXCR4 in infection with feline immunodeficiency virus.   Molecular Membrane Biology **16**:67-72.

39.   **Willett, B.J., M.J. Hosie, J.J. Callanan, J.C. Neil, and O. Jarrett**. 1993. Infection with feline immunodeficiency virus is followed by the rapid expansion of a CD8+ lymphocyte subset. Immunology **78**:1-6.

40.   **Willett, B.J., M.J. Hosie, T.H. Dunsford, J.C. Neil, and O. Jarrett**. 1991. Productive infection of T-helper lymphocytes with feline immunodeficiency virus is accompanied by reduced expression of CD4. AIDS **5**:1469-1475.

41.   **Willett, B.J., M.J. Hosie, J.C. Neil, J.D. Turner, and J.A. Hoxie**. 1997. Common mechanism of infection by lentiviruses. Nature **385**:587

42.   **Willett, B.J., L. Picard, M.J. Hosie, J.D. Turner, K. Adema, and P.R. Clapham**. 1997. Shared usage of the chemokine receptor CXCR4 by the feline and human immunodeficiency viruses. J.Virol. **71**:6407-6415.

43.   **Yamamoto, J.K., T. Okuda, C.D. Ackley, H. Louie, E. Pembroke, H. Zochlinski, R.J. Munn, and M.B. Gardner**. 1991. Experimental vaccine protection against feline immunodeficiency virus. Aids Res.Hum.Retroviruses **7**:911-921.

44.   **Yang, J.S., R.V. English, J.W. Ritchey, M.G. Davidson, T. Wasmoen, J.K. Levy, D.H. Gebhard, M.B. Tompkins, and W.A. Tompkins**. 1996. Molecularly cloned feline immunodeficiency virus NCSU1 JSY3 induces immunodeficiency in specific-pathogen-free cats. J.Virol. **70**:3011-3017.

FIGURE LEGENDS

Figure 1. Quantification of proviral load and CD4:CD8 ratio in FIV infected cats during the acute phase of infection. Three cats were inoculated intraperitoneally with either GL8$_{414}$ (O), PET$_{F14}$ (∇) or mock-infected with PBS ($\square$). (A) Proviral DNA load in PBMC was estimated by real-time PCR (control cats were consistently negative and thus are not shown). Each point represents the mean proviral load of the three cats in the group (+/- SE). (B) CD4:CD8 ratio was estimated by flow cytometry. Results represent the mean CD4:CD8 ratio of the three study groups (+/- SE).

Figure 2. Effect of FIV infection on (A) CD4+, (B) CD8+ and (C) CD8$\alpha\beta^{low}$ lymphocyte subsets. The percentage of peripheral blood lymphoid cells expressing CD4 and CD8 was quantified in each of the three study groups, GL8$_{414}$- infected (O), PET$_{F14}$-infected ($\square$) or mock-infected with PBS (∇) by flow cytometry and the absolute cell number of each subset calculated from the results of haematological analysis. Results are expressed as the mean (+/-SE) cell number (x10^9/l), * denotes significant difference (p=0.046).

Figure 3. Quantification of proviral load in FIV infected cats during the acute and chronic phases of infection. Three cats were inoculated intraperitoneally with either GL8$_{414}$ (open symbols) or PET$_{F14}$ (closed symbols) and the proviral DNA load in PBMC was estimated by real-time PCR. The sequential proviral loads of each cat in the two groups are shown as % infected PBMC.

Figure 4. Expansion of CD8$\alpha\beta$low$^+$ lymphocyte subpopulations in FIV infected cats. Contour plots of representative analyses of one cat from each group at 144 weeks post infection (CON=control 612, GL8=GL8$_{414}$-infected 612, PET=PET$_{F14}$-infected 628). Boxed regions illustrate the analysis gates for each population.
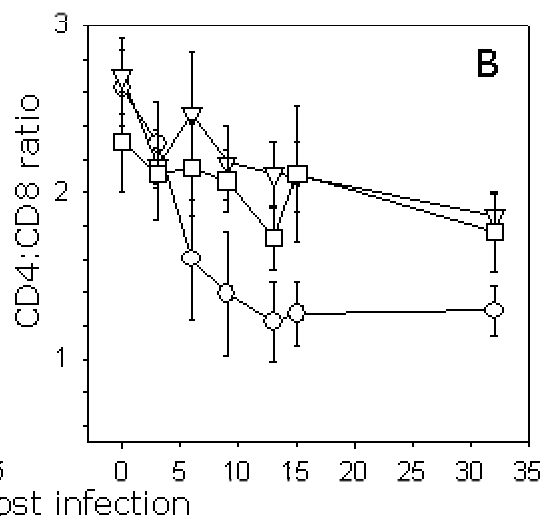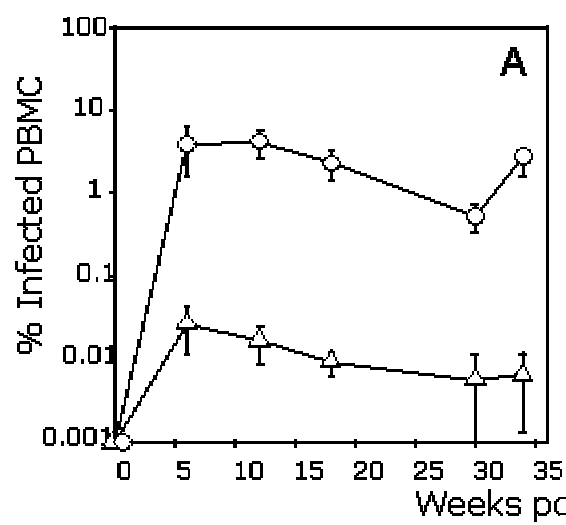

Figure 5. Predicted amino acid sequence of the V3 – V6 region of the FIV envelope glycoprotein from revertant viruses (627$_{W135}$ and 628$_{W135}$) at 135 weeks post
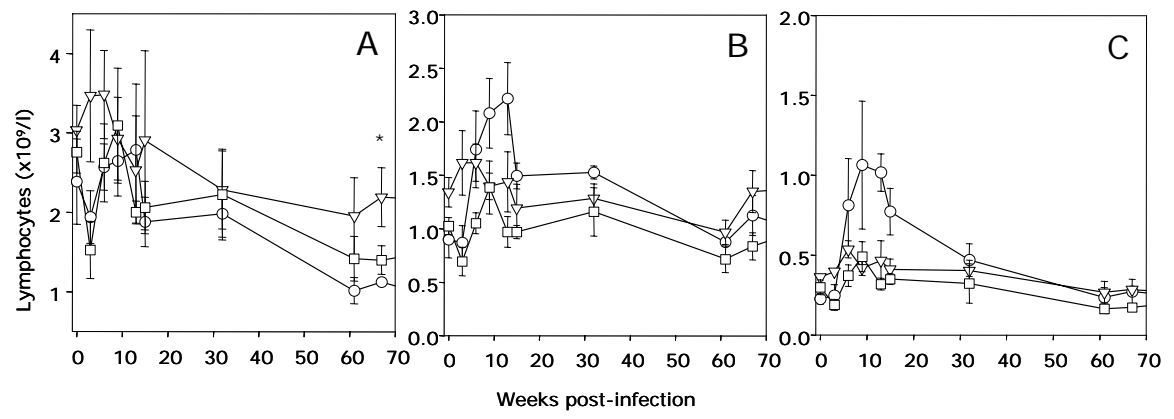
infection. Lines under the sequence delineate the variable regions 3, 4, 5 and 6. Predicted sites for N-linked glycosylation (ϕ) , and residues in the V3 loop affecting CXCR4-usage ($\downarrow$) are marked. Sequences are shown relative to the parent molecular clone PET_{F14}, and to the $GL8_{414}$ molecular clone for comparison. Sequences were consistent between three independent clones.
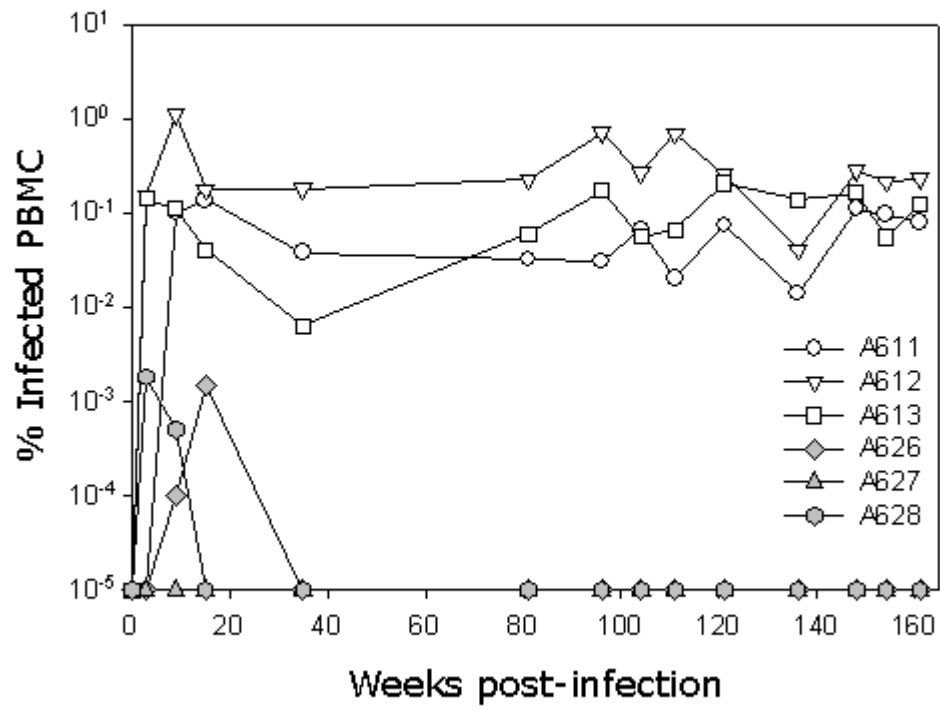
Figure 6. Reduced fusogenicity of envelope glycoproteins from 627_{W135} and 628_{W135} viruses. Env genes from PET_{F14} (a), $GL8_{414}$ (b),627_{W135} (c) and 628_{W135} (d), $GL8_{E407K}$ (e) were subcloned into the vector VR1012 and transfected into CXCR4-expressing AH927 cells. The empty vector VR1012 was transfected as a control (f.). 48 hours post-transfection the cells were fixed, stained and examined by light microscopy. Figures (a to f) illustrate representative syncytia observed with each construct. The number of syncytia per filed were enumerated, the data represent the mean number (n=5) of syncytia per field +/- SE.
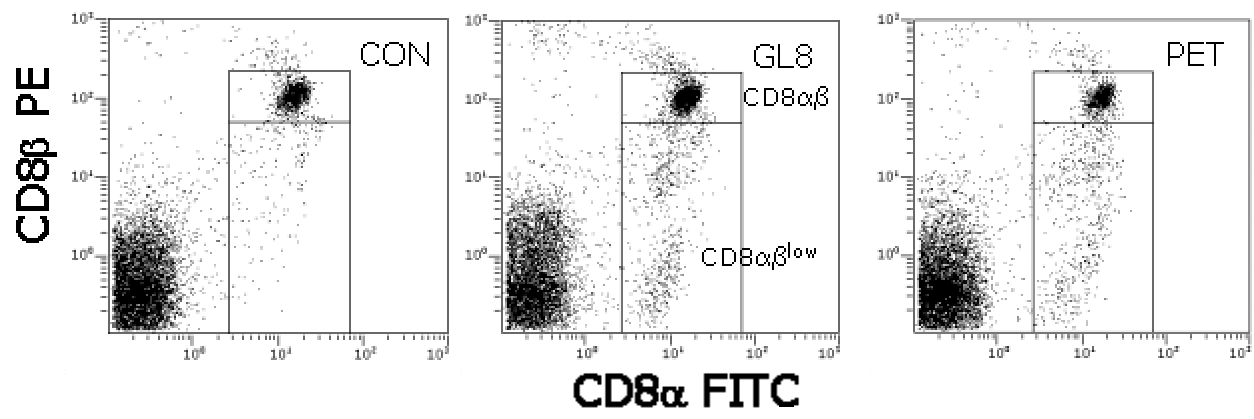
Figure 7. Impaired growth of the 627_{W135} and 628_{W135} viruses in CXCR4-expressing feline cells. PET_{F14}, $GL8_{414}$, 627_{W135} and 628_{W135} viruses were used to infect AH927 cells-expressing which had been engineered to over-express feline CXCR4.   Infection was performed in the presence (O) or absence ($\bullet$) of the CXCR4-antagonist AMD3100.   Supernatants were collected at 9 days post infection and assayed for reverse transcriptase (RT) activity. Results represent the mean of duplicate samples and are expressed as pg/ml RT.

Figure 8. Quantification of (a.) proviral load, (b.) viral load and (c.) CD8$\alpha\beta$ low in FIV infected cats during the acute phase of infection. Three cats were inoculated intraperitoneally with either PET_{F14} (O), 627_{W135} (∇) or 628_{W135} ($\square$). (a.) Proviral DNA load in PBMC was estimated by real-time PCR. Each point represents the mean % infected PBMC of the three cats in the group (+SE). (b.) Viral load in plasma was estimated by real-time PCR. Each point represents the mean number of virions per ml of plasma from the three cats in the group (+SE). (c.) Expansion of CD8βlow lymphocyte subpopulations following infection with the three isolates, expressed as CD8$\alpha\beta$low/CD8α cells. Each point represents the mean ratio of CD8$\alpha\beta$low/CD8α cells for the three cats in each group (+SE).

Figure with three panels (A, B, C) showing Lymphocytes ($\times10^9$/l) on the y-axis versus Weeks post-infection on the x-axis.

```
              351                                                        400
PET_F14       IPKCGWWWQW AYYWSCKWWW AKVKFWCQRT QSQPGSWFRA ISSWKQRWRW
628_W133      ---------- ---------- ---------- ---------- ----------
627_W133      ---------- ---------- ---------- ---------- ----------
GL8_414       ---------I ------R--S TD-------- -----L-L-- ----------
                                                          V3
              401    ↓ ↓         ●          ●                       ●50
PET_F14       EWRPDFESKK VKISLQCWST KWLTFAWRSS GDYGEVTGAW IWFGCHRWWS
628_W133      ---------E- ---------- ---------- ---------- ----------
627_W133      ---------Q- ---------- -T-------- ---------- ----------
GL8_414       ---------E- --V------- ---------- ---------- ----------

              451                     ●                             ●00
PET_F14       KLHAWARFRI RCRWWVGSWT SLIDTCGWTQ KVSGAWPVDC TWYSWKWYWC
628_W133      ---------- ---------- ---------- ---------- ----------
627_W133      ---------- ---------- ---------- ---------- ----------
GL8_414       ---T------ -------D-- -------E-- ---------- ---A-R----
                                        V4
              501                          ●                        ●50
PET_F14       SLQWGFTWKV DDLIWHFWWK KAVEWYWIAG WWSCTSDLPS SWGTWWCWCT
628_W133      ---------- ---------- ---------- ---------- ----------
627_W133      ---------- ---------- ---------- ---------- ----------
GL8_414       ---------- --------T- ---------- --------P T----------
                                                          V5
              ●51                                                   600
PET_F14       WSSSSYSGTK WACPSWRGIL RWWYWPVAGL RQSLEQYQVV KQPDYLVVPE
628_W133      ------W--- ---------- ---------- ---------- ----------
627_W133      ---------- ---------- ---------- ---------- ----------
GL8_414       ----T.WSV- ----K-Q--- ---------- -----K---- ---------G
                                                          V6
              601
PET_F14       EVWWYKPRRK RAAIHVWLAL
628_W133      ---------- ----------
627_W133      ---------- ----------
GL8_414       ---------- ----------
```